PROCEEDINGS OF SPIE

SPIEDigitalLibrary.org/conference-proceedings-of-spie

Characterization of coatings for straylight and photoluminescence suppression in the Raman Spectrometer for MMX (RAX)

Conor Ryan, Ute Böttger, Maximilian Buder, Yuichiro Cho, Sven Gutruf, et al.

Conor Ryan, Ute Böttger, Maximilian Buder, Yuichiro Cho, Sven Gutruf, Till Hagelschuer, Martin Pertenais, Andreas Pohl, Selene Routley, Friedrich Schrandt, Sergey G. Pavlov, "Characterization of coatings for straylight and photoluminescence suppression in the Raman Spectrometer for MMX (RAX)," Proc. SPIE 12188, Advances in Optical and Mechanical Technologies for Telescopes and Instrumentation V, 121884N (29 August 2022); doi: 10.1117/12.2627219

SPIE.

Event: SPIE Astronomical Telescopes + Instrumentation, 2022, Montréal, Québec, Canada

Characterization of Coatings for Straylight and Photoluminescence Suppression in the Raman Spectrometer for MMX (RAX)

Conor Ryan[a], Ute Böttger[a], Maximilian Buder[a], Yuichiro Cho[b], Sven Gutruf[c], Till Hagelschuer[a], Martin Pertenais[a], Andreas Pohl[a], Selene Routley[a], Friedrich Schrandt[a], and Sergey G. Pavlov[a]

[a]Institute for Optical Sensor Systems, German Aerospace Center (DLR), Rutherfordstraße 2, 12489 Berlin, Germany
[b]Department of Earth and Planetary Science, The University of Tokyo, 7-3-1 Hongo, Bunkyo, Tokyo 113-0033, Japan
[c]Kampf Teleskop Optics GmbH, Geisenhausener Str. 11a, 81379 Munich, Germany

ABSTRACT

The Martian Moons eXploration (MMX) mission led by JAXA to Mars moons Phobos and Deimos involves a small rover developed by DLR/CNES that will be operating on Phobos' surface. Aboard it is the Raman Spectrometer for MMX (RAX), whose main scientific objectives address Phobos surface mineralogy, its heterogeneity and relation to the Mars mineralogy. Raman spectrometers require strong suppression of straylight, since this technique operates with few nano-Watt signals that should have significant contrast to all other sources of light inside the instrument. The mission requirements involving RAX call for a compact and sophisticated optical design, precluding space for straylight suppressive elements. To optimize straylight suppression in RAX, Raman scattering, Photoluminescence and reflection were characterized for candidate coatings representing different absorbing materials and fabrication technologies over spectral ranges between 530 nm and 680 nm. This was complimented by mechanical testing to aid selection of the coatings for parts inside the RAX flight model.

Keywords: Raman Spectrometer, Absorbing Coatings, Straylight, Space Instrumentation

1. INTRODUCTION

The Martian Moons eXploration (MMX) mission led by JAXA to Mars moons Phobos and Deimos include a small rover[1] developed by DLR/CNES that will be operating on Phobos' surface. Aboard it is the Raman Spectrometer for MMX (RAX), whose main scientific objectives address Phobos surface mineralogy, its heterogeneity and relation to the Mars mineralogy. RAX is a very lightweight and highly compact Raman spectrometer with a mass of 1.5 kg and a volume of less than 1 dm^3. The spectrometer is equipped with a miniaturized and highly sensitive optical assembly, that allows measurement of weak Raman signals and enables the identification of water-bearing minerals. The RAX spectrometer is described in detail here.[2]

1.1 Raman Spectroscopy

Raman Spectrometry relies is the detection of inelastically scattered (Raman scattered) photons. In principle, a small number of the photons are reemitted from a laser-excited sample with shifted wavelengths. These photon energy differences are dependent on molecular structures and their vibrational modes, which in turn can be used for molecular identification. Raman signals (RS), which comprise of these photons, are weak because the Raman scattering cross-section is very small compared to elastic scattering of the laser. Due to the typical Raman scattering efficiency for inorganic solids below 1e-6, Raman responses acquired by the RAX instrument are expected not exceeding a few nano-Watts.

Further author information: (Send correspondence to C. Ryan)
E-mail: conor.ryan@dlr.de

Advances in Optical and Mechanical Technologies for Telescopes and Instrumentation V, edited by Ramón Navarro, Roland Geyl, Proc. of SPIE Vol. 12188, 121884N
 · 0277-786X · doi: 10.1117/12.2627219

A laser signal must arrive at the detector for measurement of wavelength shift. The laser signal should be attenuated to the below the intensity of the Raman signal, to maximize exploitation of the dynamic range of the detector. A so-called Stokes shifted Raman emission contains photon energy downshifted from the laser. Due to the downshift, the laser signal should occupy one extreme end of the detector array, while the other extreme limits the measurable spectral range. The spectral range of the Raman signal is determined by the deterministic bands of inorganic solids, that can be limited to ca. 3800 cm^{-1} in Stokes shift, making the spectral range of interest for RAX between 532 nm and 667 nm. Raman scattering emission usually consists spectrally of some discrete lines / bands, distributed over 100s of nm. It can be anisotropic and therefore with favorable directions, especially for crystalline solids.

1.2 Photoluminescence

Laser excitation is also accompanied by broadband photoluminescence (PL) due to decay of excited electron states. PL is emitted with downshifted photon energy too and overlaps spectrally with Raman emission. Spectrally resonant enhancement or very efficient luminescent materials could contaminate the useful Raman signal. Therefore, prior characterization of Raman and PL responses of absorbing coatings is necessary procedure in the selection of the appropriate material and fabrication technology. PL is a material dependent emission, which is non-directional and spectrally broadband for most minerals, although particular metal ions (e.g. rare-earth) have discrete atomic-like emission spectra

1.3 Straylight

Straylight refers to any unintended light in an optical system. It can be light from an unintended source, or an intended source on an unintended path. Straylight from the high-powered laser source is thought to be a major risk to the function of the RAX Raman spectroscope, owing to the potential ten orders of magnitude difference between the source laser power and that of the gathered Raman signal. Even the slightest contamination of the Raman signal by inadvertently gathered or scattered laser light can be ruinous owing to this magnitude difference. This leads to two functions of the optical design of a Raman spectrometer. Firstly, direction of correctly attenuated laser light with the Raman signal into the spectrometer slit. This is achieved with a combination of focusing optics and filters in the beam path and is explained elsewhere,[3] where ca. 6-7 orders of magnitude of laser signal are removed. Secondly, prevention of all other straylight from reaching the detector with significant intensity. Since the instrument's detector is sensitive from the UV-A to the near-infrared (NIR) range, any non-laser light over this wide spectral range may pass RAX's filters and thus contribute to distortion of the Raman signal.

Straylight produced inside the instrument has several sources: specular and diffuse reflections, Rayleigh scattering, photoluminescence and Raman scattered emission. Reflections and scattering of the unfiltered laser light are somewhat directional but also contribute to a background level of light in the whole instrument. External straylight sources such as backscattered laser light from the measured sample (Phobos regolith in the case of RAX Science measurements), sunlight and other instruments must be considered. Backscattered laser light contains encoded information about the surface morphology,[4] but is noise for the purpose of spectral measurement. To minimize the straylight intensity arriving at the detector, several strategies are pursued in parallel. In the context of the MMX Rover, Raman measurements are taken in the shadow of the rover, during Phobos "night". The RAX design implements baffles and screens, anti-reflection coatings on optics and blackening of mechanical surfaces. In addition, using the grating substrate as a total internal reflection (TIR)-waveguide for unwanted diffraction modes of the grating was used to transport light away from the field of view (FOV) of the camera. The beam path from slit to detector in a grating-based spectrometer should be fully enclosed. This limits the number of straylight sources which can be "seen" directly by the detector. The non-optical surfaces in the enclosure should suppress straylight, since any straylight created within this enclosure may interact with these surfaces multiple times before arriving at the detector.

1.4 RAX Design

The optical layout of the RAX Spectrometer is shown below (Fig. 1). Light from the excitation laser enters the system through a fiber, and straylight from the laser source and fiber is filtered out by the laser cleanup

filter. The remaining excitation light is collimated before being focused onto a spot on the sample with the autofocus system. Due to the confocality of the fiber tip, spot-on-sample and slit, spectral filtering is the only way to reduce the laser signal beyond the slit. A dichroic beam splitter reflects the Raman shifted light to the laser quelling filter, which in combination attenuates remaining laser light by between six and seven orders of magnitude. The combined signal is passed through the slit, which is imaged onto the detector via the grating. The detector is a 12-bit 2048x2048 CMOS Camera with space heritage from 3D Plus.

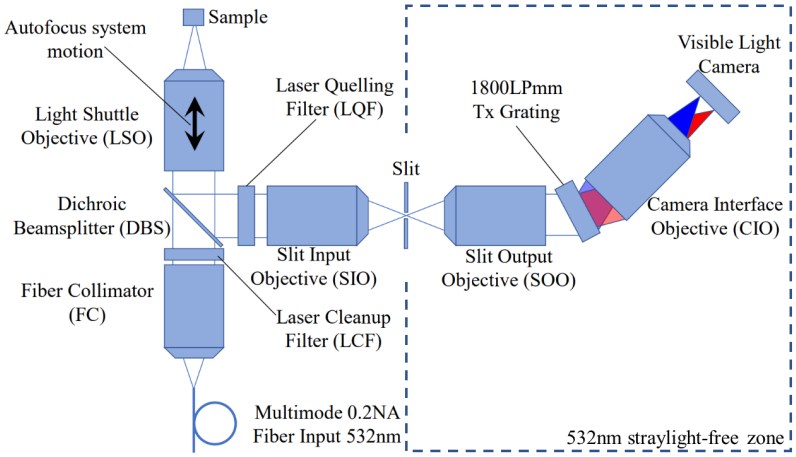

Figure 1. Optical Layout of the RAX Raman Spectrometer – Source: 3

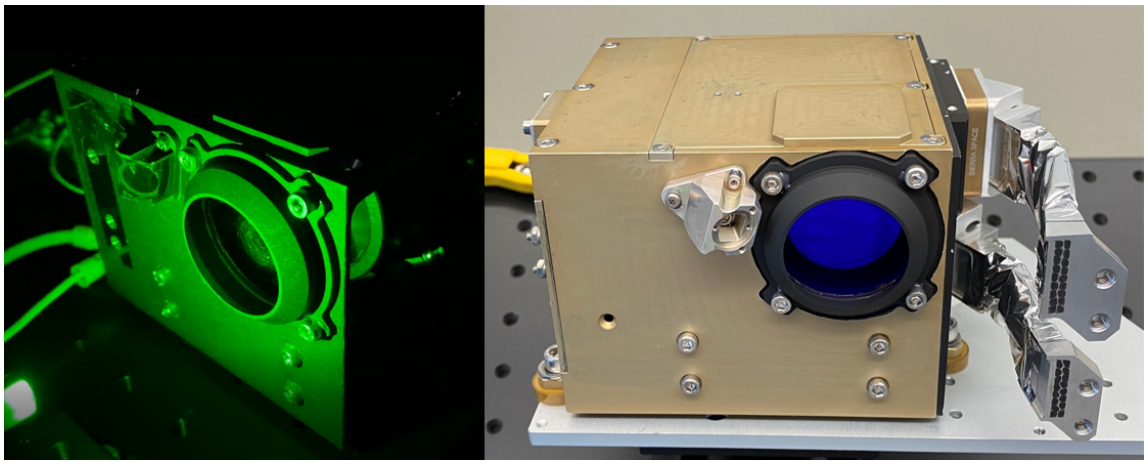

Figure 2. Left: RAX Spectrometer Module illuminated by backscatter of an impinging 40mW laser light beam on the sample. A cover was removed to view resulting straylight inside instrument. Right: RAX Spectrometer Module under laboratory illumination.

1.5 Black Coating Requirements

Only a partial enclosure of the slit-detector optical path was possible due to the extremely compact design and motion of the autofocus system. Hence all possible surfaces needed to be blackened to suppress the background level of straylight in the instrument. A selection of anti-straylight coatings was needed for opto-mechanical and structural components. The blackened surfaces are required to have the following optical properties: low reflection, low photoluminescence (PL) and low Raman scattering (RS) under incident 532nm light. Suppression of PL and Raman emissions are important because if the coating creates particulates during integration, these can travel to areas of high laser intensity in the beam path. From there, the PL and Raman straylight signals

can travel unfiltered to the detector. Other relevant characteristics are the suitability of blackened surfaces for gluing, thermal and electrical conduction, the thickness of the surface layer, the robustness of the surfaces against damage. A quantitative characterization of the optical properties of twenty-six coating samples was performed, before testing of some mechanical properties of select candidates.

2. METHOD

2.1 Samples

Table 1 lists the coatings, suppliers, substrate materials and preparation. In total 26 samples are presented. Samples were typically a few cm's in size and in some cases required holes or uncoated sections to allow for a particular coating process. Primarily aerospace grades of Aluminium and Titanium alloys were tested, since these are the main substrates of interest in the RAX instrument. Since thick oxide layers such as KEPLA-COAT coatings are electrically and thermally isolating, coated parts are often masked in some areas, leaving the masked surfaces uncoated. For space applications, it is advised in ECSS standards to passivate all surfaces. A second coating for conductive passivation of Aluminium can be achieved with Surtech or Alodine coatings, which were tested in this report. These produce very thin passivating layers, which can be produced more simply in Titanium alloys with anodization.

2.2 Optical Testing Methods

2.2.1 Raman and Photoluminescence Measurements

The Raman measurements were performed with a confocal Raman microscope Witec alpha300R system at the DLR Institute for Planetary Research, Berlin. The Raman spectrometer operates with the same laser excitation wavelength as the RAX spectrometer, 532 nm, and the same optical configuration, confocal. The spectral resolution is 10 cm^{-1}. A Nikon 10 x objective was used with a given spot size in focus on the samples of about 1.5 μm. Spectra were taken at 3 mW, 5 mW and 7 mW which then equals to 5.3 mW/μm^2, 8.8 mW/μm^2 and 12.4 mW/μm^2 laser irradiation on the sample, respectively. Ten spectra were taken at each sample point with an integration time of 2 seconds per spectrum and subsequent averaging. Microscopy images were taken with varying illumination to produce similar contrasts.

2.2.2 Reflection Measurements

Several coating samples were delivered with relevant information on semispherical reflectivity of coating in visible spectral range (see Table 1). Reflectivity of the coatings were characterized using bi-directional diffuse reflectance measurements with a Bruker Fourier Transform Vertex 80v spectrometer in the visible to near-infrared range (480 – 1200 nm). The diagnostic light spot on a sample had a diameter of 6 mm for the incident (α) and reflection (β) angles $\alpha = \beta = 13°$. While bi-directional reflection measurements are less representative for characterization of stray light than semi-spherical absorption, they permit direct comparison of various coatings used in this study.

2.2.3 Mechanical Tests

A cross-cut tape test according ISO 2409:2007. An adhesion test with ScotchWeld Epoxy 2216 was performed by gluing M3 screws to the blackened surface and comparing the tensile forces required to break the cured bond. The tensile force as well as the breakage location were compared to that of control samples.

3. RESULTS

3.1 Carbon-based black coatings

The optical properties of the light-absorbing, carbonaceous substance often called "black carbon" or "carbon black", depend on molecular form, particularly the size of sp^2-bonded clusters (e.g. in planar layers of graphite), while sp^2-bonds are diamond-like characteristic features.[5] We have studied two types of carbon-based absorbing materials: diamond-like carbon coatings (a class of amorphous carbon material that displays some of the typical properties of diamond, due to mixed sp^2 bonded carbon atoms together with sp^3 bonds) as well as carbon nanotubes (one of the allotropes of carbon, a two-dimensional hexagonal lattice of carbon atoms, i.e. entirely sp^2 bonded, rolled up along one of the Bravais lattice vectors of the hexagonal lattice to form a hollow cylinder).

Table 1. Black coating samples, sorted by substrate material

Abbreviation for paper	Trade Name, Standard or Specification	Coating Supplier	Substrate	Pre-coating surface treatment
MagicBlack-Al-SB	MagicBlack ™	ACM Coatings GmbH, Germany (subsidary of Acktar Ltd.)	Aluminium-alloy unknown at date of publication	sandblasted
Alumite-Al-chem	Alumite	Nittoh Inc., Japan	Aluminium-EN AW 6061 (3.3214)	chemical roughening
Kepla/Alodine-Al	KEPLA-COAT ™ 20 Black (10µm) and Alodine 1200	Aalberts Surface Technologies, Germany Frühschütz Lohngalvanik, Germany	Aluminium-EN AW 7075 (3.4365)	blank
Kepla/Surtech-Al	KEPLA-COAT ™ 20 Black (10µm) and Surtech 650	Aalberts Surface Technologies, Germany	Aluminium-EN AW 7075 (3.4365)	blank
Kepla-Al	KEPLA-COAT ™ 20 Black (10µm)	Aalberts Surface Technologies, Germany	Aluminium-EN AW 7075 (3.4365)	blank
Kepla-AlSi	KEPLA-COAT ™ 20 Black (10µm)	Aalberts Surface Technologies, Germany	Aluminium Alloy AlSi42-CE13	blank
Metalvelvet	MetalVelvet ™	ACM Coatings GmbH, Germany (subsidary of Acktar Ltd.)	foil-composition unknown at date of publication	-
FractalBlack-SST-SB	FractalBlack ™	ACM Coatings GmbH, Germany (subsidary of Acktar Ltd.)	Stainless steel-alloy unknown at date of publication	sandblasted
Vacuumblack-SST-SB	VacuumBlack ™	ACM Coatings GmbH, Germany (subsidary of Acktar Ltd.)	Stainless steel-alloy unknown at date of publication	sandblasted
Kaniblack-ST	Kaniblack ™ 10µm	Japan Kanigen Co., Ltd., Japan	Steel-cold rolled (1.0330)(SPCC according to JIS)	blank
Grey-Ti	based on AMS2488 Type 2	Viktor Hegedüs GmbH, Germany	Titanium-Grade 2 (3.7035)	blank
Grey-Ti-etched	based on AMS2488 Type 2	Viktor Hegedüs GmbH, Germany	Titanium-Grade 2 (3.7035)	blank, acid clean 1 minute
Grey-Ti-polished	based on AMS2488 Type 2	Viktor Hegedüs GmbH, Germany	Titanium-Grade 2 (3.7035)	polished without acid clean
Grey-Ti-SB	based on AMS2488 Type 2	Viktor Hegedüs GmbH, Germany	Titanium-Grade 2 (3.7035)	sandblasted without acid clean
Blue-Ti	AMS2248 Type 3	Poligrat Deutschland, Germany	Titanium-Grade 5 (3.7165)	blank
Blue-Ti-SB	AMS2248 Type 3	Poligrat Deutschland, Germany	Titanium-Grade 5 (3.7165)	sandblasted
DLC-Ti	Diamond-Like Carbon	Kuhn Beschichtungen GmbH, Germany	Titanium-Grade 5 (3.7165)	blank
DLC-Ti-matte	Diamond-Like Carbon	Kuhn Beschichtungen GmbH, Germany	Titanium-Grade 5 (3.7165)	"matte black finish"
DLC-Ti-SB	Diamond-Like Carbon	Kuhn Beschichtungen GmbH, Germany	Titanium-Grade 5 (3.7165)	sandblasted
Kepla/Surtech-Ti	KEPLA-COAT ™ 20 Black (15µm) and Surtech 650	Aalberts Surface Technologies, Germany	Titanium-Grade 5 (3.7165)	blank
Kepla-Ti	KEPLA-COAT ™ 20 Black (15µm)	Aalberts Surface Technologies, Germany	Titanium-Grade 5 (3.7165)	blank
Kepla-Ti-Acetone	KEPLA-COAT ™ 20 Black (15µm)	Aalberts Surface Technologies, Germany	Titanium-Grade 5 (3.7165)	blank, wiped with acetone after
Kepla-Ti-SB	KEPLA-COAT ™ 20 Black (15µm)	Aalberts Surface Technologies, Germany	Titanium-Grade 5 (3.7165)	sandblasted
Laserblack-Ti	Laser Black ™	Epner Technology Inc, USA	Titanium-Grade 5 (3.7165)	blank
Poligrat-Ti	Poligrat Grey (LB 139/20 Var. 1a, 2a (Grey))	Poligrat Deutschland, Germany	Titanium-Grade 5 (3.7165)	blank
Poligrat-Ti-SB	Poligrat Grey (LB 139/20 Var. 1a, 2a (Grey))	Poligrat Deutschland, Germany	Titanium-Grade 5 (3.7165)	sandblasted

3.1.1 CVD-deposited Carbon nanotube coatings

Carbon nanotubes have been shown to behave similarly to a black body,[6] with strong broad-band absorbance and a similar spectrum to carbon black and graphite. This occurs for the vertically aligned single-walled CNT absorbers, when light occurs to be “trapped” between the tubes due to multiple reflections. Space qualified black coatings from Acktar Ltd. (Israel) offer broad-band (UV-VIS-NIR) low reflectivity (semi-spherical at low incident angles not exceeding 0.01-0.02) and low emissivity together with high adhesion to metallic surfaces and mechanical sustainability.[7] The manufacture characterizes it as a layer of carbon nanotubes (CNTs) that

comprise metal oxide claddings that sheathe the carbon nanotubes. The metal oxide claddings are preferably transparent and conformal with the CNTs. The manufacturer lists different possible material selections for this cladding. The carbon-nanotube-based composite coating is typically porous. The CNT-based composite coatings are fabricated using a low-temperature chemical vapor deposition (CVD). The CNTs are preferably non-aligned (i.e. entangled), thus forming an (isotropic) CNT thicket that ensures absent directionality to the incident light.[8]

Under a 5 mW 532 nm excitation, the Acktar coatings deliver the RS and PL signals with mean intensities following the order of the magnitude of their specified reflectance, i.e. the lower reflectivity corresponds to the lower RS+PL signals. The lowest values are measured for the thinner coatings, Metal Velvet™and Magic Black™. One may assume that number of defects causing PL increases with the CNT volume.

The carbon-nanotube (CNT)-based composite coatings do not demonstrate typical CNT Raman and PL spectra. This is apparently a result of entangled spatial ordering of CNTs, reducing all light signals. MgO is expected to be a dominant cladding phase. While most of materials for oxide claddings listed by the manufacturer have a large bandgap, several of materials have the energy gaps falling into visible, where most of Raman lasers operate. Moreover, optical properties of such oxides on low-dimensional CNT are modified, so that for instance vanadium oxide thin films may have bandgaps of about 2.32 eV [9], which is in resonance with the green Raman laser (532 nm = 2.33 eV). The observed Raman feature - broad band(s) between 800 cm^{-1} and 900 cm^{-1} that are seen Figure 3, could be assigned e.g. to amorphous V_xO_x overlaping bands at ca. 800 cm^{-1} (V_2O_3) and 880 cm^{-1} (VO_2).[10] This means that one should take care to select materials for the cap layers in order to avoid resonant enhancement of the Raman effect, that could increase Raman response on orders of magnitude.

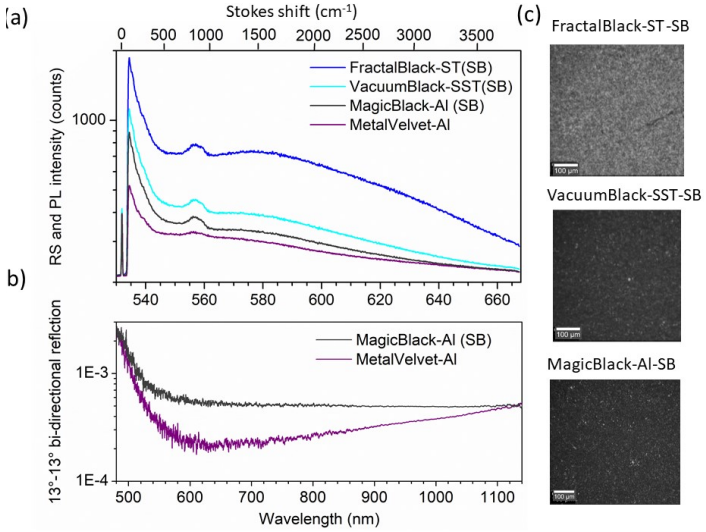

Figure 3. (a) Typical Raman spectra of CNT black coatings covered by composite metal oxides from Acktar Ltd. Taken at 5 mW of 532 nm laser excitation. (b) Bi-directional reflection spectra for two coatings with the lowest RS+PL response. (c) Images of the coatings under the Raman microscope. The white bar is 100 μm.

In a view of potentially weak Raman and PL signals and very low reflectivity, these coatings are candidates for the space Raman spectrometers. Despite the oxide cladding, these coatings are known to be fragile to contact with hard surfaces. These coatings were deemed unusable for almost all components in the compact and complex RAX assembly, due to the risk of multiple contacts during integration.

3.1.2 Diamond-like Carbon black coatings

Diamond-like carbon (DLC) coatings combine outstanding properties of diamond (as structural) and carbon (optical). They can be deposited either with PVD (Physical Vapor Deposition; physical gas phase deposition about by evaporation or sputtering) or CVD (Chemical Vapor Deposition) gas phase methods. The DLC black coatings from KUHN Beschichtungen GmbH demonstrate clear black carbon Raman features (amorphous carbon

Bands D and G at ca. 1310 cm^{-1}, ca. 1600 cm^{-1} respectively) on top of moderate PL signal (Figure 4). With increase of roughness of the coating surface (blank → matte finishing → abrasive blasting) the PL signal drops while Raman signal does not change much. Generally, carbon-based coatings require special treatment of metallic surface or deposition of buffer layers (like SiC, CN^x, $SiSiN_x$[11]) for the sufficient adhesion. Also pure DLC films exhibit large internal compressive stress that often released by/into morphology: scratches and similar. These coatings were not considered for the RAX instrument, reflection measurements were skipped.

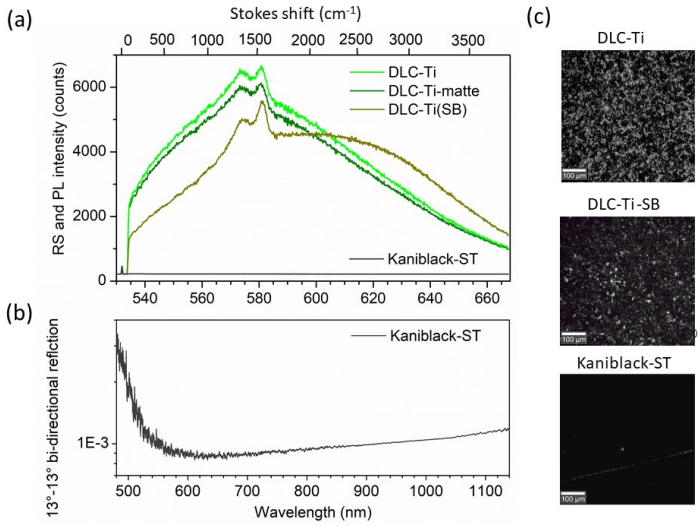

Figure 4. (a) Typical Raman spectra of DLC coatings with different treatments after deposition on Ti substrates from KUHN-Beschichtigung GmbH: blank – as deposited, matte – matte finishing, sandblasted – abrasive blasting. Kaniblack-ST is Ni-P alloy black coating on steel substrate from Japan Kanigen Co., Ltd. (b) Bi-directional reflection spectra of Kaniblack-ST coating. (c) Images of the coatings under Raman microscope. Scratch on the KaniBlack-ST coating is due to handling.

3.1.3 Black Ni-P alloy coatings

Nickel–Phosphorus (Ni-P) alloys may be chemically treated (etched) to produce black coatings ('Ni–P black') that can act as very efficient light absorbers. The main components of the black coating are recognized to include NiO, Ni_2O_3 and some nickel phosphate.[12] The Ni–P black surfaces exhibit, as a rule, a very low specular reflectance, for instance less than 0.4% at 633 nm.[12]

The Kaniblack® coatings from Japan Kanigen Co., Ltd. are plated and etched on cold-rolled low-carbon steel substrates using an electroless plating process. The coatings demonstrate very low reflectance (Figure 4), b) and vanishing Raman and PL responses. Based on the sample in this report, they appear to be fragile and sensitive to handling.

3.1.4 Metal-oxide black anodized coatings: dominating amorphous phase

Electrolytic passivation process, used to increase the thickness of the natural oxide layer on the surface of metal parts, is broadly used for building black absorbing coatings at metallic surfaces, such as Aluminum (Al), Titanium (Ti), Magnesium and alloys. Among anodizing acids, sulfuric and chromic are as the major anodizing contenders. Black anodic films of inorganic dyes are low cost, resistant against corrosion, and have relatively low risk of contamination of spacecraft's instruments, for instance by outgassing or multi-elemental pollution.[13] From a technical point of view, an anodic film is not an additional coating but a conversion interface tightly bound to the metallic parent substrate. This implies natural adhesion of anodic films to metallic surfaces. Since both Ti and Al are widely used for space instrumentation construction/housing, anodization is a natural way of forming black coatings. For aerospace applications, AMS (Standard Aerospace Material Specification) Type II and Type III anodizations are common for Ti-alloys.

KEPLA-COAT® from Aalberts Surface Technologies GmbH are advanced anodic plasma-chemical surface finishes. The processing leads to oxide ceramic layers, which offer, in addition to standard high wear and corrosion protection, also a uniform layer structure and temperature resilience. The KEPLA-COAT coatings are multi-layer structures, having a high-pore-count ceramic cap layer and a low pore-count oxide ceramic layer with a 100 nm barrier layer as interface to the aluminum or titanium alloy substrates.[14]

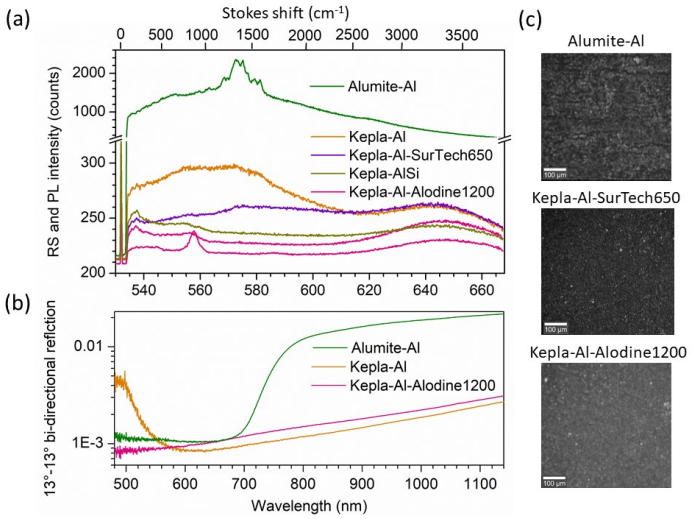

Figure 5. (a) Typical Raman spectra of anodic plasma-chemical KEPLA-COAT black coatings from Aalberts Surface Technologies on Al alloys, also with different alodine treatment; anodic oxidation of Al alloy from Nittoh Inc. Taken at 5 mW of 532 nm laser excitation. (b) Bi-directional reflection spectra of selected coatings. (c) Images of the Alumite-Al and KEPLA-COAT black coatings on Al substrates.

Raman / PL spectra of KEPLA-COAT coatings on aluminum alloys have a weak-to-vanishing Raman feature of a black carbon (amorphous carbon bands D and G at ca. 1310 cm^{-1}, ca. 1600 cm^{-1} relatively) and a weaker broad band at around 3330 cm^{-1} (probably C-H band) on top of weak PL signal (Figure 5). Passivation of the coating on Al alloy substrate by chromate conversion (alodine coating) reduces the PL signal.

Anodized coating on aluminum alloy 6061 (AlMgSi) from Nittoh Inc., Japan, (Alumite in Figure 5) exhibits low reflection in visible range, but significant Raman (possibly black carbon - like) and PL signals.

KEPLA-COAT on Titanium (Ti-6Al-4V) substrates deliver expressed band centered at ca. 636 cm^{-1} (Figure 6) that could be assigned to titania (TiO_2) films (possibly also in a nanotube form).[15] Sand-blasted finish of Ti substrate has a negligible effect on intensities of Raman and PL signals of coating. Some reduction of Raman and PL occured in samples recoated with SurTech 650 (Figure 6). All KEPLA-COAT coatings exhibit very low reflection in VIS-NIR spectral ranges.

It should be highlighted here that the effects on part geometry are quite different for Kepla-Ti- variants and Kepla-Al- variants. With Titanium substrates, the produced oxide layer grows entirely on the surface, while with aluminium substrates, it diffuses into the substrate as well. As an example, the diameter change of an internal hole may be over 50µm for Kepla-Ti but less than 10µm with Kepla-Al. This must be considered when applying KEPLA-COAT at interfaces for mating parts.

The coatings from Poligrat Deutschland GmbH obtained by electrolytically-carried anodic oxidation on grade 5 (Ti6Al4V) titanium demonstrate weak Raman signals on the low PL background in short-wavelength visible spectral range. The coating process is modified from AMS Type-II and the main feature – band at ca. 630 cm^{-1} apparently indicates on formation of amorphous titania (TiO_2). AMS2248 Type-III blue-anodization coatings exhibit lower photoluminescence but larger VIS-NIR reflection. Sand-blasted finishing of Ti substrates modifies the intensity of PL signals and changes spectral characteristics in visible range (Figure 7).

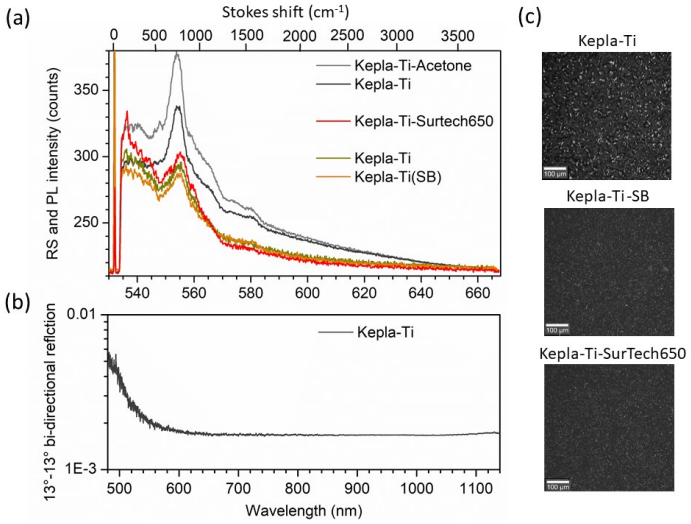

Figure 6. (a) Typical Raman spectra of anodic plasma-chemical KEPLA-COAT black coatings from Aalberts Surface Technologies on Ti alloys, also with different treatment of substrate and coating. Taken at 5 mW of 532 nm laser excitation. (b) Bi-directional reflection spectra of selected coatings. (c) Images of the KEPLA-COAT black coatings on Ti substrates.

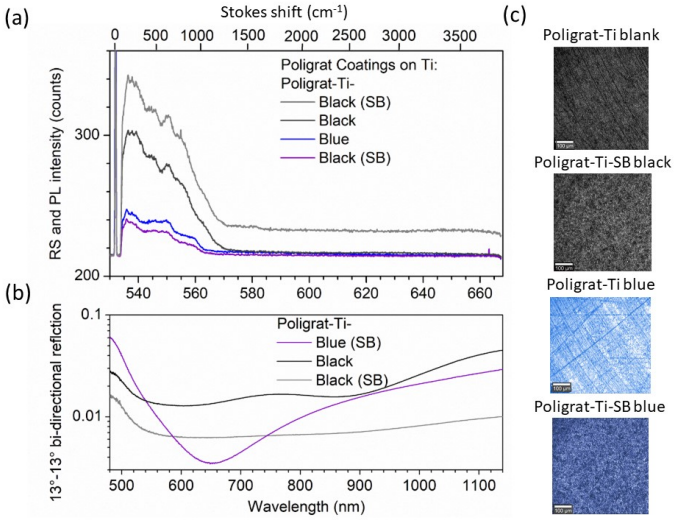

Figure 7. (a) Typical Raman spectra of anodic black and blue coatings from Poligrat Deutschland GmbH on Ti alloys. Taken at 5 mW of 532 nm laser excitation. (b) Bi-directional reflection spectra of selected coatings. (c) Images of the black and blue coatings on Ti.

3.1.5 Metal-oxide black anodized coatings: crystalline phases

Several techniques of catalytic black coatings are apparently resulting in formation of metallic oxides in crystalline phase, that would cause significant distortion of acquired Raman spectra and which is not desired for Raman spectrometers. For instance, dark anodizing of titanium and alloys based on AMS 2488 Type II utilized by Viktor Hegedüs GmbH, reveal black coatings with presence of rutile (titanium dioxide (TiO_2) in ditetragonal form) with Raman bands at ca. 252 cm^{-1}, 433 cm^{-1} and 615 cm^{-1} (Figure 8). These coatings were precluded from usage in the RAX spectrometer due to significant reflectance.

Epner Technology Flat Black Coating (Laser Black) is a multi-layer metallic oxide formed mainly from duplex copper coating, giving a velvet-like copper oxide, that can be convert also into a darker color. According to the

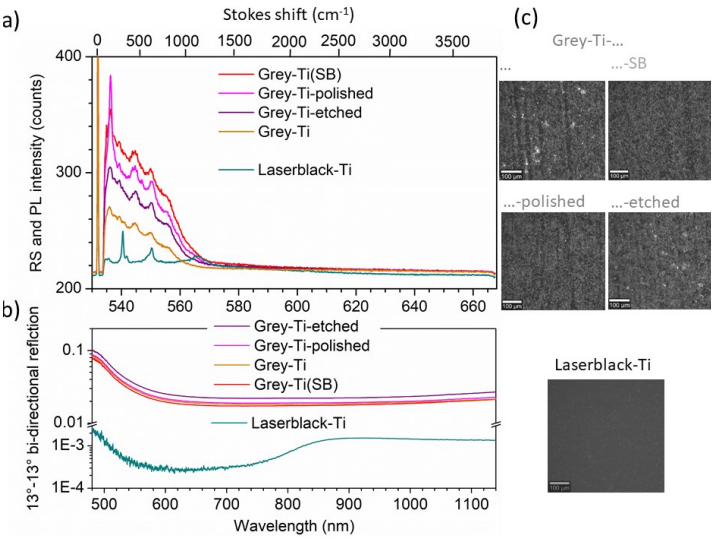

Figure 8. (a) Typical Raman spectra of anodic black coatings with distinct fingerprints of crystalline phase. Taken at 5 mW of 532 nm laser excitation. (b) Bi-directional reflection spectra of selected coatings. (c) Images of the black coatings on Ti.

supplier, the spherical reflection in visible range is below 0.015 while it increases steeply up to 0.045 towards near-infrared.[16] Our reflection measurements confirm very low reflectivity of the Laser Black coating in Figure 8. Raman spectra reveal clear spectral features (ca. 296 cm^{-1}, 343 cm^{-1} and 628 cm^{-1}) of bulk CuO (mineral tenorite) if compared with calculated active phonon zone-centered modes in 17. Other copper oxide configurations are apparently either not formed or at much lower density. The supplier notes a "somewhat fragile" surface of the coating. Like Acktar coatings, they are suitable only for applications where risk of contact with other objects is extremely low.

An overview table of the optical measurement results is given in Table 2. For readability, colour scales in a spectrum from green (good) to red (poor) were added indicating black coating performance in RS and PL reflection. The RS and PL classifications and colour shading indicates the threshold exceeded by any part of the the RS and PL spectrum measured, excluding the laser line at 532 nm. "High" has exceeded 1000 counts, while "medium", "low" and "very low" are completely below 1000 counts, 400 counts and 300 counts respectively. Similarly, the colour scale on bi-directional reflection at 532 nm change colour at threshold values of 0.2, 1.5 and 3 percent.

3.2 Mechanical Properties and Tests

The mechanical testing was focused on the qualification of KEPLA-COAT for blank Aluminium alloy 7075 and Titanium Grade 5 (Kepla-Al and Kepla-Ti). Table 3 is a summary table of the mechanical testing results. The tensile force required to break the Epoxy Bond between KEPLA-COAT samples and the stainless steel screw were found to be the same as for the control samples (Poligrat anodized Titanium). The breakage occurred at the coating/epoxy interface for Kepla-Al and in the screw/epoxy interface for Kepla-Ti. In neither case was damage visible to the coating of any KEPLA-COAT samples.

At the time of ordering the coatings of the flight-model components, the mechanical impact of coating process interactions had not yet been tested. Previous models were built with single coatings only. A pairing of KEPLA-COAT and Surtech was planned, but there was a compatibility issue between the aluminium alloy EN-AW 7075 and the Surtech 650 coating. Therefore Alodine 1200 was selected late in the project to be paired with KEPLA-COAT. Unfortunately, it was found during the spectrometer build that the Alodine process had increase the fragility of the black KEPLA-COAT coating. Coatings of ISO Class 0 to ISO Class 1 are recommended for space applications. ISO Class 2 was accepted for the instrument due to schedule pressure. This highlights the need to specify and test alloy and coating combinations in parallel during early design phases, so the experience can be

Table 2. Overview of optical test results of black coating samples, sorted by substrate material

Abbreviation for paper	Absorber	RS + PL	Bi-directional Reflection at 532nm
MagicBlack-Al-SB	CNT / ceramic cap layer	medium	0.0007765
Alumite-Al-chem	Black aluminum oxide	high	0.00111
Kepla/Alodine-Al	Black aluminum oxide / Chromium passivation Alodine 1200 (yellow)	very low	0.000884
Kepla/Surtech-Al	Black aluminum oxide / Chrome-free passivation SurTech 650 TCP (colorless)	very low	not measured
Kepla-Al	Black aluminum oxide	very low	0.00149
Kepla-AlSi	Black aluminum oxide	very low	not measured
Metalvelvet	CNT / ceramic cap layer	medium	0.0004466
FractalBlack-SST-SB	CNT / ceramic cap layer	high	not measured
Vacuumblack-SST-SB	CNT / ceramic cap layer	high	not measured
Kaniblack-ST	Nickel-Phosphorus alloy	very low	0.00110
Grey-Ti	Black Titanium oxide	very low	0.03552
Grey-Ti-etched	Black Titanium oxide	low	0.04262
Grey-Ti-polished	Black Titanium oxide	low	0.03672
Grey-Ti-SB	Black Titanium oxide	low	0.03324
Blue-Ti	Blue Titanium oxide	very low	not measured
Blue-Ti-SB	Blue Titanium oxide	very low	0.01713
DLC-Ti	Amorphous carbon	high	not measured
DLC-Ti-matte	Amorphous carbon	high	not measured
DLC-Ti-SB	Amorphous carbon	high	not measured
Kepla/Surtech-Ti	Black Titanium oxide / Chrome-free passivation SurTech 650 TCP (colorless)	low	not measured
Kepla-Ti	Black Titanium oxide	very low	0.002365
Kepla-Ti-Acetone	Black Titanium oxide	low	not measured
Kepla-Ti-SB	Black Titanium oxide	very low	not measured
Laserblack-Ti	Black Copper oxide	very low	0.000498
Poligrat-Ti	Black Titanium oxide	low	0.0150
Poligrat-Ti-SB	Black Titanium oxide	low	0.00773

gained with flight-like coatings, avoiding late changes. This is recommended even where experience exists with an alloy and coating, as changing supplier processes and regulatory restrictions will impact the end result.

Table 4 shows the coatings implemented in the flight version of the RAX spectrometer. Due to supplier time constraints and their prior positive experience with the coating, a decision was made to accept Alumite coating before test results were available.

At the time of publication, the characterization of the flight-model optical performance is not complete. An impression of straylight levels in the flight-model can nonetheless be gained from the Raman measurements taken

Table 3. Results of mechanical tests on selected black coatings

Sample	Designed Surface Thickness [µm]	Adhesion Test Result		Suitability for Epoxy 2216 gluing
		according to ASTM D3359	according to ISO Classification	
Kepla-Al	10 µm ± 5 µm	3B	2	OK
Kepla-Ti	15 µm ± 5 µm	3B	2	OK
Kepla/Alodine-Al	10 µm ± 5 µm	3B	2	untested

Table 4. Final black coating selection in the RAX Spectrometer

Coatings used on RAX-FM optomechanics
Aluminium Alloys
KeplaCoat Black 10µm, blank
Alumite, chemical roughening
Titanium Alloys
KeplaCoat Black 15µm, blank
Poligrat-Black, sandblasted
Iron (Steel) Alloys
Black Nickel plating

during thermal-vacuum testing of the flight-model. As an example, Figure 9(a) shows a raw image from the detector while RAX is measuring Olivine. The vertical direction corresponds to spectral distribution and the horizontal axis to spatial distribution along the spectrometer slit. Raman features are seen as small dots amongst the vertical stripe of fluorescence, while the laser line is visible as the small horizontal line and dot at the bottom of the image. The area encompassing these features is the region of interest used to produce Raman spectra. By enhancing the contrast for low-light regions of the raw image, one can see an almost uniform background straylight level well below the level of light in the region of interest. A straylight artefact can be seen near the laser line in (b). It is possibly a ghost reflection of the laser spot, but irrelevant since it is outside the region of interest. Finally, reading out the raw values of the pixels in a column passing through the Raman features shows (c) a clear Raman spectrum from a single uncorrected image. The impression is that the instrument appears to be unimpinged by straylight.

4. CONCLUSION

Straylight comes from sources internal and external to a Raman spectrometer, and consists of light with the laser excitation wavelength but also other wavelengths. Straylight mitigation by design consists of two elements – physically screening straylight from the detector and reducing overall straylight levels by applying absorptive coatings to optomechanical components. For a space-bound Raman spectrometer, the optical requirements are low RS and PL and low reflection. In addition, electrical, thermal and mechanical requirements must be considered. For development of the RAX Spectrometer, an array of absorptive coatings were optically tested, with the best candidates undergoing mechanical tests. Most of the black coating technologies offer high light absorption. For the coating materials of amorphous inorganic matter, there is often the following trend: the lower is reflectivity, the lower is the RS and PL signal. Amorphous materials exhibit generally weaker and broader Raman scattering fingerprints then crystalline solids. The techniques resulting in formation of solids with crystalline phases, yield distinct Raman fingerprints and therefore cannot be recommended for Raman spectrometers. The lowest reflection occurs from the nanostructured surfaces where light appears to be caught in the coating by multi-reflection. Caution should be taken if the nanostructures are fragile. Sand-blasting prior to coating increases the proportion of diffuse reflection while reducing specular reflection. It has varying effects on photoluminescence levels, depending on the coating process. While the Alodine process was not detrimental to optical performance of KEPLA-COAT on Aluminium alloy 7075, it was detrimental to the mechanical robustness

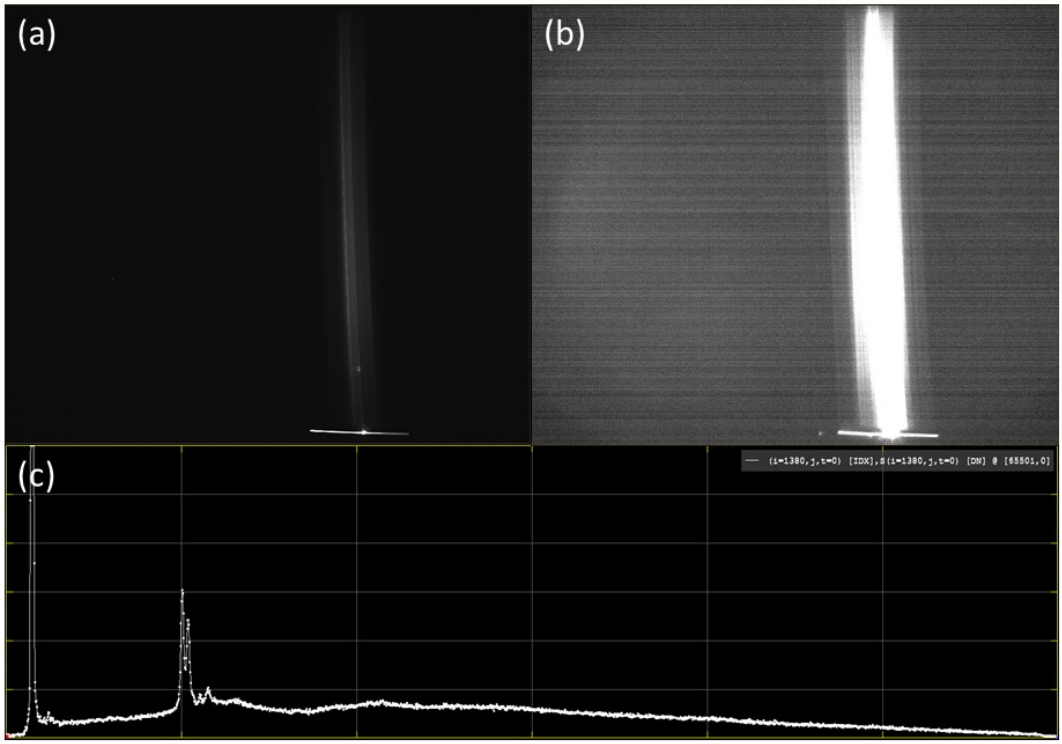

Figure 9. (a) Unprocessed detector image during Raman measurement of Olivine at -40°C. (b) Contrast of (a) manipulated to highlight variations between low-light pixels. (c) Plot of pixel column of (a) dissecting a Raman feature.

of the coating. For compact Raman spectrometers, KEPLA-COAT was found to be a suitable coating for Aluminium alloy 7075, while KEPLA-COAT Black, Epner Laserblack and Poligrat Grey were (optically) all suitable black coatings for Titanium alloys and Ni-P coatings were found suitable for steel. Coatings in the RAX Spectrometer were chosen on this basis and a preliminary evaluation of flight model straylight levels is promising.

ACKNOWLEDGMENTS

The authors thank all companies listed in this report for advice and assistance in supplying samples as well as the Institute for Planetary Research at DLR, Berlin for the possibility to use their Raman microscope and Laboratory.

REFERENCES

[1] Michel, P., Ulamec, S., Böttger, U., Grott, M., Murdoch, N., Vernazza, P., Sunday, C., Zhang, Y., Valette, R., Castellani, R., et al., "The MMX rover: performing in situ surface investigations on Phobos," *Earth, Planets and Space* **74**(1), 1–14 (2022).

[2] Cho, Y., Böttger, U., Rull, F., Hübers, H.-W., Belenguer, T., Börner, A., Buder, M., Bunduki, Y., Dietz, E., Hagelschuer, T., et al., "In situ science on Phobos with the Raman spectrometer for MMX (RAX): preliminary design and feasibility of Raman measurements," *Earth, Planets and Space* **73**(1), 1–11 (2021).

[3] Rodd-Routley, S., Belenguer, T., Böttger, U., Buder, M., Cho, Y., Dietz, E., Hagelschuer, T., Hübers, H.-W., Kameda, S., Kopp, E., et al., "Optical design and breadboard of the Raman spectrometer for MMX-RAX," in [*52nd Lunar and Planetary Science Conference*], (2548), 1923 (2021).

[4] Ryan, C., Schröder, S., Gensch, M., Frohmann, S., and Dietz, E., "Optical access to the morphology of areas probed by rover-based LIBS, Raman or Fluorescence spectroscopy: first considerations," in [*43rd COSPAR Scientific Assembly. Held 28 January - 4 February*], **43** (Jan. 2021).

[5] Bond, T. C. and Bergstrom, R. W., "Light Absorption by Carbonaceous Particles: An Investigative Review," *Aerosol Science and Technology* **40**(1), 27–67 (2006).

[6] Mizuno, K., Ishii, J., Kishida, H., Hayamizu, Y., Yasuda, S., Futaba, D. N., Yumura, M., and Hata, K., "A black body absorber from vertically aligned single-walled carbon nanotubes," *Proceedings of the National Academy of Sciences* **106**(15), 6044–6047 (2009).

[7] Acktar Ltd., "Acktar Black - World's Blackest Coatings." https://www.acktar.com/wp-content/uploads/2017/10/Acktar_brochure.pdf. (accessed: 20 June 2022).

[8] Bahlawane, N., "Carbon-nanotube-based composite coating and production method thereof." https://patents.google.com/patent/WO2017001406A2/en (2017). (Patent: WO2017001406A2).

[9] He, Q., Xu, X., Gu, Y., Wang, M., Yao, J., Jiang, Y., Sun, M., Ao, T., Lian, Y., Wang, F., and Li, X., "Vanadium oxide–carbon nanotube composite films characterized by spectroscopic ellipsometry," *Journal of Physics D: Applied Physics* **49**(40), 405105 (2016).

[10] Shvets, P., Dikaya, O., Maksimova, K., and Goikhman, A., "A review of Raman spectroscopy of vanadium oxides," *Journal of Raman spectroscopy* **50**(8), 1226–1244 (2019).

[11] Lee, K.-R., Yong Eun, K., Kim, I., and Kim, J., "Design of W buffer layer for adhesion improvement of DLC films on tool steels," *Thin Solid Films* **377-378**, 261–268 (2000).

[12] Brown, R. J. C., Brewer, P. J., and Milton, M. J. T., "The physical and chemical properties of electroless nickel–phosphorus alloys and low reflectance nickel–phosphorus black surfaces," *J. Mater. Chem.* **12**, 2749–2754 (2002).

[13] Goueffon, Y., Arurault, L., Mabru, C., Tonon, C., and Guigue, P., "Black anodic coatings for space applications: Study of the process parameters, characteristics and mechanical properties," *Journal of Materials Processing Technology* **209**(11), 5145–5151 (2009).

[14] Aalberts Surface Technologies, "Anodising." https://www.aalberts-st.com/processes/anodizing/. (Accessed: 21 June 2022).

[15] Zhao, J., Wang, X., Chen, R., and Li, L., "Fabrication of titanium oxide nanotube arrays by anodic oxidation," *Solid State Communications* **134**(10), 705–710 (2005).

[16] Epner Technology Inc., "Diffuse Reflectance of Laser Black on Thick Substrate." https://www.epner.com/wp-content/uploads/2014/11/Diffuse-Reflectance-of-Laser-Black-on-Thick-Substrate.pdf. (Accessed: 21 June 2022).

[17] Debbichi, L. , Marco de Lucas, M. C., Pierson, J. F., and Krüger, P., "Vibrational Properties of CuO and Cu_4O_3 from First-Principles Calculations, and Raman and Infrared Spectroscopy," *J. Phys. Chem. C* **116**(18), 10232–10237 (2012).